Cloud Publications
International Journal of Advanced Earth Science and Engineering
2016, Volume 5, Issue 1, pp. 347-363, Article ID Sci-388
ISSN: 2320 – 3609

Research Article | Open Access

Evaluation of Clearness and Diffuse Index at a Semi-Arid Station (Anantapur) using Estimated Global and Diffuse Solar Radiation

Rama Gopal K.[1], Pavan Kumari S.[1], Balakrishnaiah G.[1], Raja Obul Reddy K.[1], Md. Arafath S.[1], Siva Kumar Reddy N.[1], Chakradhar Rao T.[1], Lokeswara Reddy T.[1], and Reddy R.R.[1,2]

[1]Aerosol & Atmospheric Research Laboratory, Department of Physics, Sri Krishnadevaraya University, Anantapur, Andhra Pradesh, India
[2]Srinivasa Ramanujan Institute of Technology, B.K. Samudram Mandal, Anantapur, Andhra Pradesh, India

Publication Date: 12 April 2016

Article Link: http://scientific.cloud-journals.com/index.php/IJAESE/article/view/Sci-388

Abstract In the present study, collocated and simultaneous measurements on meteorological parameters and solar radiation on horizontal surface were obtained from different meteorological sensors and pyranometer sensor over a semi-arid station, Anantapur (14.62° N, 77.65° E and 331 m asl) during January–December 2013. The temperature is usually lower at midnight, decreasing in the early hours of the morning around 08:00 LT (Local Time) (24.71 ± 2.7 °C), and then increasing rapidly until just after midday at 15:00 LT (31.88 ± 3.2 °C). It decreases to 26.70 ± 2.9 °C during the night around 23:00 LT. The relative humidity ranges from 30–76%, 20–65%, 46–80% and 48–90% during winter, summer, monsoon, and post-monsoon seasons respectively. The diurnal variation of soil moisture exhibits slight variations at different depths over the region. The diurnal and monthly variations of solar radiation as well as clearness index (k_t), diffusion index (k_d) were studied in the present study. In diurnal variation, it shows a steady rise in solar radiation received at the surface after 7:30 LT and attains a maximum solar radiation between 12:00 – 13:00 LT. The amount of solar radiation also varies depending on the time of day and the season. The annual mean of daily global, extraterrestrial and diffuse radiation at Anantapur is found to be 202.43 ± 40.45, 408.15 ± 61.63 and 49.33 ± 11.26 W/m^2. The high global and diffuse solar radiations were observed during March-May (257.67 ± 34.18 W/m^2, 65.07 ± 11.20 W/m^2) whereas low global and diffuse solar radiations during monsoon months (137.66 ± 12.41, 33.47 ± 7.44 W/m^2). In the case of extraterrestrial solar radiation was high in the month of December (472.92 ± 0.67 W/m^2) and low in the month of June (312.87 ± 2.58 W/m^2).

Keywords *Global Solar Radiation; Diffuse Solar Radiation; Extra Terrestrial Solar Radiation; Clearness Index; Diffuse Index*

1. Introduction

The air temperature variation brings about a change in water evaporation and air saturation and leading to the change in air humidity. Furthermore, the air temperature differences between different

locations will also cause air pressure differences, which in turn would produce air movement, thereby wind. This variation in humidity and wind speed leads to direction affect on rainfall. Thus, all weather variations on the Earth are more or less affected by each other. Two components of global solar radiation come to the earth surface are from the sun i.e. one is direct solar radiation and the other originates from dispersing of direct solar radiation in the atmosphere i.e. diffuse solar radiation. The radiation that reflects from surroundings (so-called albedo) is of importance for some angle to the horizontal surface. This radiation is mainly diffuse and comes to the receiving surface under different angles. Solar radiation is received at the earth's surface under different atmospheric conditions, which clearly affect the amount and quality of radiation obtained at the ground. Turbidity, transparency, air mass, atmospheric water vapor contents layers and distribution of cloud cover have been suggested as the atmospheric conditions that exert influence solar radiation at the earth's surface through the process of absorption, scattering and reflection of the incoming solar radiation. Clearness index (k_t) is expressed as the ratio of the monthly mean daily global solar radiation on the horizontal surface to the monthly mean daily extraterrestrial horizontal radiation. Clearness index indicates the availability of global solar radiation at a particular location. The diffuse fraction of solar radiation (the ratio of the diffuse solar radiation to the global solar radiation) is particularly required in assessing the climatologically potential of a locality for solar energy utilization and in estimating the expected values of the output of concentrating solar collectors [1].

In this paper, the diurnal and monthly average total of extraterrestrial radiation, global solar radiation, diffuse solar radiation, clearness index (k_t) and diffuse index (k_d) in Anantapur are analyzed. In addition, a frequency distribution of clearness index and diffuse index of global solar radiation are also presented and discussed.

2. Instrumentation and Site Description

Mini Boundary Layer Mast (MBLM) has been established across the country with broad objective to characterize and analyse the region wise specific surface layer structures in terms of surface roughness, the bulk coefficients for surface fluxes, similarity coefficients and the scaling laws for surface transports, etc., for varying stability conditions. The Mini Boundary Layer Mast is a 15 m high, guyed, uniform triangular lattice structure designed to withstand wind speed of 60 m/s. The system uses advanced high resolution sensors to measure the ambient temperature, relative humidity and wind vector. The booms on MBLM are fitted at 4 m, 8 m and 15 m heights above the ground. The system uses advanced high resolution sensors to measure ambient temperature, relative humidity and wind vector at three different levels at 4.0 m, 8.0 m and 15 m. In addition to this it will measure rainfall, net incoming solar radiation in long wave and short wave range, atmospheric pressure, soil temperature at seven levels and soil moisture at six levels. All the data are collected at one second resolution and averaged for every four minutes. The data are stored in a local data logger as well and can be downloaded using a USB drive. The system shall be useful to study the boundary layer process at fine scale. The details of experiment facility and the instrumentation were discussed by [2].

2.1. Description of Study Area

Anantapur district in Rayalaseema region of Andhra Pradesh is geographically situated in a semi-arid zone and occupied the second place to Rajasthan. Anantapur is a very dry semi-arid and rain shadow region. The region gets very little rain that from during South-West monsoon and North-East monsoon periods. The observation site (14.62°N, 77.65°E and 331 masl), Sri Krishnadevaraya University (SKU) is situated at about 12 km away from the southern edge of the Anantapur town (Figure 1). This region receives very little rainfall and the average annual rainfall was around to the 313.5mm.Within a 50 km radius, this region is surrounded by a number of cement plants, lime kilns, slab polishing and brick making units.

The study area is also at a relatively short distance from the national highways (NH 7 and NH 205) and the diesel vehicles and biomass burning to cause the air pollution. Based on different meteorological conditions prevailing over the observation site, the months of the year are classified into four seasons namely winter (December-February), summer (March-May), monsoon (June-August) and post-monsoon (September-November). The climate here is primarily hot and dry in the summer, hot and humid during the monsoon and post monsoon and dry in winter season.

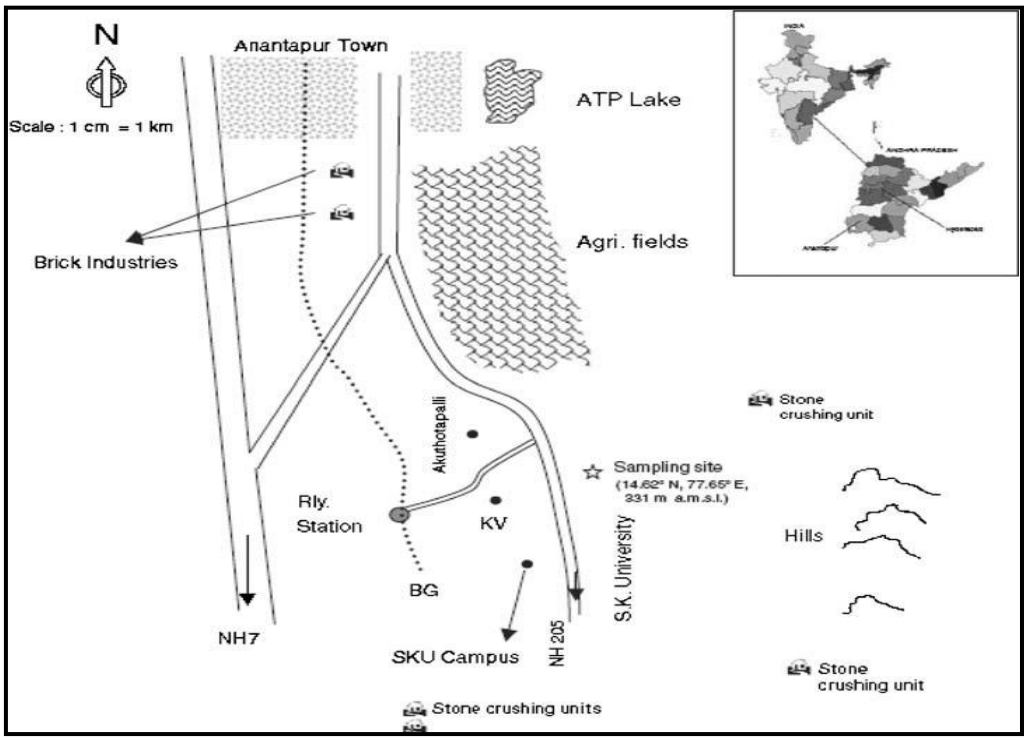

Figure 1: *Location map of the Anantapur city in India*

2.2. Extraterrestrial Radiation for Hourly or Shorter Periods (H_o)

For hourly or shorter periods the solar time angle at the beginning and end of the period should be considered when calculating H_o:

$$H_o = \frac{12(60)}{\pi} G_{SC} d_r [(\omega_2 - \omega_1)\sin(\varphi)\sin(\delta) + \cos(\varphi)\cos(\delta)(\sin(\omega_2) - \sin(\omega_1))] \quad (1)$$

Where
H_o extraterrestrial radiation in the hour (or shorter) period [$MJm^{-2}hour^{-1}$], G_{sc} solar constant = 0.0820 $MJm^{-2}min^{-1}$, d_r inverse relative distance Earth-Sun, φ latitude (rad) δ solar declination (rad), ω_1 solar time angle at beginning of period (rad), ω_2 solar time angle at end of period (rad),

The solar time angles at the beginning and end of the period are given by:

$$\omega_1 = \omega - \frac{\pi t_1}{24} \quad (2)$$

$$\omega_2 = \omega + \frac{\pi t_1}{24} \quad (3)$$

Where
ω solar time angle at midpoint of hourly or shorter period (rad), t_1 length of the calculation period (hour): i.e., 1 for hourly period or 0.5 for a 30 minute period.

The solar time angle at midpoint of the period is:

$$\omega = \frac{\pi}{12}[(t + 0.06667(L_z - L_m) + S_c) - 12] \quad (4)$$

Where
't' standard clock time at the midpoint of the period (hour). For example for a period between 14:00 and 15:00 hours, t = 14.5, L_z longitude of the centre of the local time zone (degrees west of Greenwich).

For example, L_z = 75, 90, 105 and 120° for the Eastern, Central , Rocky Mountain and Pacific time zones (United States) and L_z = 0° for Greenwich, 330° for Cairo (Egypt) and 255° for Bangkok (Thailand), L_z = 82.5° for India. L_m longitude of the measurement site (degree west of Greenwich), S_c seasonal correction for solar time (hour).

The seasonal correction for solar time is:

$$S_c = 0.1645\sin(2b) - 0.1255\cos(b) - 0.025\sin(b) \quad (5)$$

$$b = \frac{2\pi(J - 81)}{364} \quad (6)$$

Where J is the number of the day in the year.

2.3. Diffuse Solar Radiation for Daily Periods

The total solar radiation consists of direct or beam radiation coming directly from the solar disc and the diffuse component scattered to the ground from the sky dome. The latter depends on the clarity of the sky and could be estimated from the correlation of (Collares-Pereira and Rabl, 1979) which gives the daily average diffuse radiation, $H_{d|}$ as:

$$H_d = H\{0.775 + 0.0060(\omega_S - 90) - [0.505 + 0.00455(\omega_S - 90)]\cos(115k_t - 103)\} \quad (7)$$

Where k_t is the clearness index for the day, defined as the ratio of the daily radiation (H) on a horizontal surface to the daily extraterrestrial radiation (H_o) on that surface, that is:

$$k_t = \frac{H}{H_o} \quad (8)$$

Its measure of the availability of the solar radiation or the transmissivity of the atmosphere.

The hourly values of the diffuse solar radiation can be estimated from the equation by (Liu and Jordan, 1960) which gives:

$$I_d = H_d \frac{24}{\pi} \frac{\cos(\omega) - \cos(\omega_S)}{\sin(\omega_S) - \frac{\pi\omega_S}{180}\cos(\omega_S)} \quad (9)$$

2.4. The Diffuse Index (k_d)

K_d is the diffuse index for the day, defined as the ratio of the daily diffuse radiation (H_d) on a horizontal surface to the daily global solar radiation (H) on that surface, that is:

$$k_d = \frac{H_d}{H} \quad (10)$$

This is the transmission characteristics of diffuse solar radiation and hence mirrors the effectiveness of the sky in transmitting diffuse solar radiation.

3. Results and Discussion

3.1. Diurnal Variation of Meteorological Parameters

Based on different meteorological conditions prevailing over the observation site, the months of the year are classified into four seasons namely winter (December-February), summer (March-May), monsoon (June-August) and post-monsoon (September-November). The diurnal and monthly variations of average temperature, relative humidity, and atmospheric pressure are shown in Figure 2 (a) - (d) and statistical data are presented in Table 1. Figure 2 (a) illustrates that the temperature is usually lower at midnight, decreasing in the early hours of the morning around 08:00 LT (Local Time) (24.71 ± 2.7 °C), and then increasing rapidly until just after midday at 15:00 LT (31.88 ± 3.2 °C). It decreases to 26.70 ± 2.9 °C during the night around 23:00 LT. The noontime values are mostly due to the high intensity of solar radiation reaching the earth's surface. Figure 2 (a) reveals that the relative humidity is usually high at midnight and in the early morning 7:00 LT (75%), drops rapidly, after the sun rises until it is lowest just after midday around 15:00 LT (40%). It increases again at midnight, rapidly in the late afternoon and early evening and levels off around midnight.

Monthly variation of temperature and relative humidity are shown in Figure 2 (c). From Figure 2 (c) it is found that the temperature increases with the decreasing of relative humidity and vice versa. The minimum temperature of 25.28 ± 3.7 °C was observed during the January 2013 and a maximum of 32.68 ± 3.6 °C during May 2013. The temperature recorded in the study area ranged between 31.95 °C – 19.37 °C, 38.24 °C – 24.21 °C, 32.25 °C – 23.82°C and 30.09 °C – 21.19 °C during the winter, summer, monsoon, and post-monsoon respectively. The relative humidity ranges observed during winter, summer, monsoon, and post-monsoon are 30 – 76%, 20 – 65%, 46 – 80% and 48 – 90% respectively. The minimum relative humidity observed in summer was 23% and a maximum of 88% during post-monsoon seasons.

Atmospheric pressure is the total weight of the air above the unit area at the point where the pressure was measured. The semi diurnal variation of atmospheric pressure was shown in Figure 2 (b) and which indicates a significant semi diurnal variation with a morning peak around 07:00 – 09:00 LT with a pressure value of 968 hPa and a minimum of 963 hPa at 16:00 LT. As the air warms up the molecules in the air become more active and they rise up with more individual space, even though there is the same number of molecules. It leads to increase in the air pressure. When the temperature cools, the molecules slow down and they do not move and bump into each other, it causes a decrease in air pressure. The Figure 2 (d) illustrates the monthly variation of pressure and the

maximum pressure was observed during the winter months (970 hPa) due to stronger confinement by the nocturnal boundary layer, which would be very shallow in the winter months due to low night temperature and minimum pressure (962 hPa) was recorded in the monsoon months due to the high winds, which are originating from the Arabian Ocean. The variations of wind speed (WS) and wind direction (WD) for the study period are shown in Figure 3 (a). Apart from the wind speed, wind direction also plays a vital role in determining the type of aerosols present over the location as they help in bringing and identifying aerosols from different neighboring regions to the measurement site. The maximum wind speed has been found to be 4 ± 0.9 m/s in the monsoon months and minimum values are found to be 1.79 ± 0.6 m/s during the post-monsoon months. From Figure 3 (a) wind directions are variable for different months of a year, i.e., winds are confined to 240^0 - 270^0 (South-easterly) during the monsoon months, 90° - 135° (Northeasterly or South-easterly) during the winter seasons, 90° - 270° during the summer and the post-monsoon months over the study area. Surface wind vectors slowly change their direction towards southwesterly during summer and post-monsoon seasons.

Therefore, during these seasons, aerosols over the observation site will have a possible influence on the marine air masses coming from the Arabian Sea [3], [4], [5]. The average monthly variation of rainfall (RF) during the study period was shown in Figure 3 (b). The maximum average rainfall was observed in the month of September (171.4 mm) and minimum during the summer months (7.3 mm). The seasonal rainfall was recorded to be 206.8, 89.1, 8.2 and 7.3 mm in the post monsoon, monsoon, winter and summer seasons, respectively. This region receives very little rainfall and the average annual rainfall was around to the 313.5 mm.

Table 1: *The Monthly Average Values of the Meteorological Parameters (mean ± SD) for the Study Period at Anantapur*

Month	Wind Speed (m/s)	Wind Direction (degree)	Temperature (°c)	Relative humidity (%)	Pressure (hPa)	Rainfall (mm)
Jan	2.06±1.03	125.92±37.30	25.283±3.71	51±16	970± 1.47	0
Feb	2.63±1.08	124.70±21.00	26.91 ±3.43	49±14	969±1.56	8.2
Mar	2.53±1.17	132.32±29.96	29.84±3.66	36±11	968±1.57	0
Apr	2.05±0.49	205.86± 30.34	32.74±3.82	36±13	964±1.72	2.5
May	2.84±0.38	242.24±20.32	32.68±3.64	45±13	961±1.25	4.8
Jun	3.25±0.88	256.33±8.26	28.26±2.53	62±10	962±1.12	9.9
Jul	3.28±0.99	254.64±6.71	27.00±2.15	67±08	963±1.31	29.4
Aug	2.96±0.87	262.18±10.98	26.92±2.30	67±09	964±1.39	49.8
Sep	1.77±0.58	243.40±10.30	26.38 ±2.32	76±10	965±1.35	171.4
Oct	1.71±0.68	226.53±24.34	26.46±2.01	73±09	969±1.56	32.6
Nov	1.89±0.87	119.72±25.63	25.15±2.66	67±13	968±1.32	2.8
Dec	2.17±0.97	125.24±32.14	23.54±3.14	57±13	969±1.40	2.1

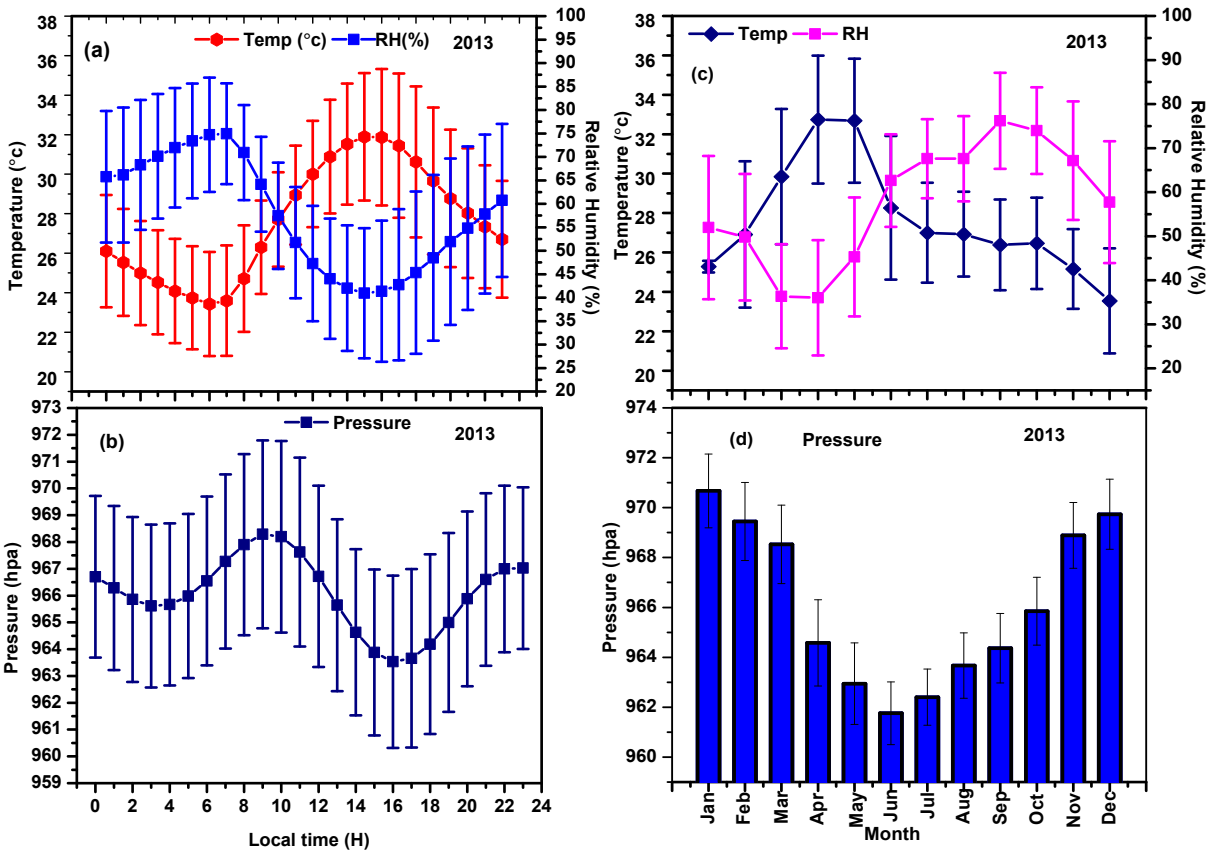

Figure 2: *Diurnal variation of (a) temperature and relative humidity (RH) (b) pressure and monthly variation of (c) temperature and relative humidity (d) pressure for the period of January – December 2013*

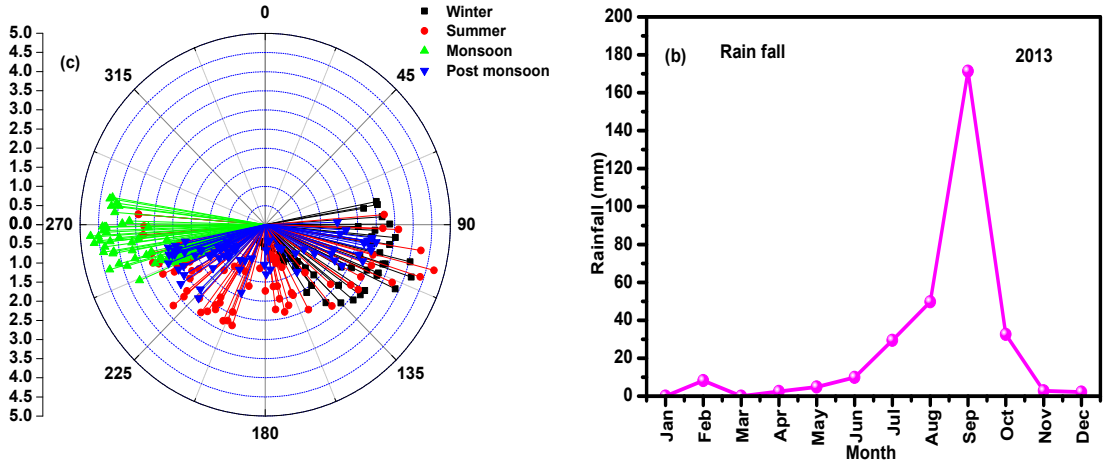

Figure 3: *Diurnal and monthly variations of (a) wind speed (WS), wind direction (WD) and (b) rain fall for the entire study period*

3.2. The Diurnal Variation of Soil Temperature and Soil Moisture for Different Depths

Soil temperature is widely used for the estimation of the soil conditions whether it is hot or cold and also it controls many chemical and biological processes within the soil. The diurnal variation of soil temperature at different depths (0cm, 5cm, 10cm, 40cm and 100cm) are shown in Figure 4 (a).

In the diurnal variation of soil temperature, the maximum value was observed during 15:00 LT due to the high temperature. After the noon time onwards the soil temperature decreased and reaches a minimum value at morning hours 06:00 LT and is due to the reduction of sun radiation and increase relative humidity and low atmospheric temperature. The similar diurnal variation of soil temperature at different depths was reported by [6]. Some interesting features will happen in the soil which involves the temperature flow of heat and how soils make heat up. In other words, the amount of heat the soil absorbs and makes to increase the soil temperature. In the first case, heat in the soil flows from places of high temperature to a low temperature so heat can move into the deeper layers of the soil profile.

Soil moisture is a key variable in controlling the exchange of water and heat energy between the land surface and the atmosphere through evaporation and plant transpiration [7]. The Figure 4 (b) shows the diurnal variation of soil moisture for different depths. The spatial structure of soil moisture and its evolution in time is both cause and consequence of vegetation [8]. The diurnal variation reaches its minimum around 8:00 LT and maximum around 16:00 LT. it is observed that soil water content varied greatly in the rainy season and less in the dry season. It is natural to suspect that this pattern might be greatly related to precipitation and evaporation. The diurnal variations at 40 and 100 cm depths do not have obvious changes in 3 contrasts to shallow layer. A similar variation in soil moisture is also reported by [9], [10].

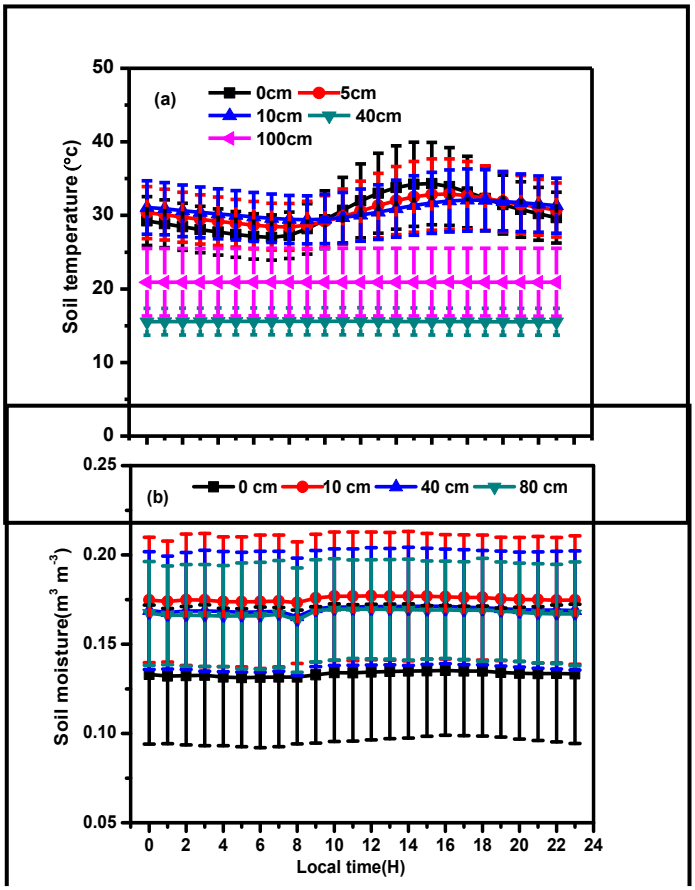

Figure 4: *Diurnal Variation of (a) Soil Temperature and (b) Soil Moisture for Different*

3.2.1. *Diurnal and Monthly Variation of Short Wave and Long Wave Solar Radiation*

The Figures 5 (a) (b) shows the diurnal and monthly variation of short wave and long wave solar radiation at Anantapur over a study period. Shortwave radiation (visible light) contains a lot of energy

and long wave radiation (infrared light) contains less energy than shortwave radiation. Solar energy enters into the atmosphere as shortwave radiation in the form of ultraviolet (UV) rays (the ones that give us sunburn) and visible light. The earth is much cooler, but still emits radiation. The radiation emitted from the earth as long wave radiation because it contains a smaller amount of energy. From the Figures 5 (a), (b) the incoming short wave solar radiation values observed were positive and outgoing long wave solar radiation values were negative. The incoming solar radiation varies from 0 W/m^2 (minimum) to about 723.56 W/m^2 (maximum). It showed maximum (723.56 W/m^2) value at noon (12:00 LT) and minimum (16.52 W/m^2) in the morning (06:00 – 07:00 LT) and evening (18:00 – 20:00 LT) (187.39 W/m^2). Similarly, the outgoing long wave solar radiation showed the negative magnitude (−91 W/m^2) at noon, indicating the high emissivity compared to morning and evening hours. The highest values of solar radiation at short and long wavelengths were recorded to be 312.87 ± 79.66 W/m^2 and -91.31 ± 20.9 W/m^2 in the month of March whereas lowest values were found to be 180.29 ± 44.3 W/m^2 and -34.14 ± 5.08 W/m^2 in the month of July respectively. In the winter time, sunshine duration was shorter than summer, but the radiation was higher than summer and in the case of rain season which was lower becomes the radiation is due to the rainy cloud.

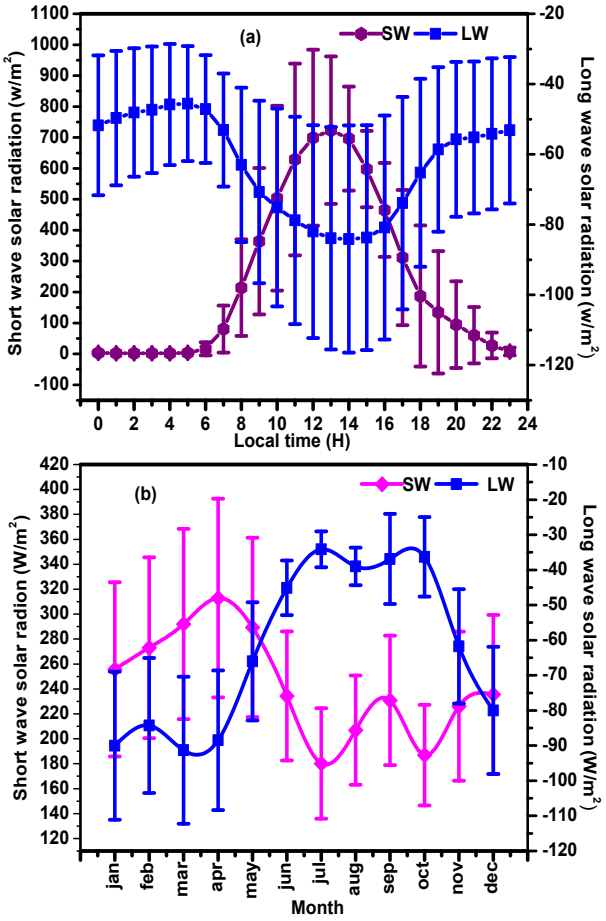

Figure 5: *Diurnal Variation of (a) Short Wave and Long Wave Solar Radiation and (b) Monthly Variation Short Wave and Long Wave Solar Radiation*

3.3. Diurnal Variation of Extraterrestrial (H_o), Global (H) and Diffuse Solar Radiation (H_d)

The Figures 6 (a), (b), (c) shows the diurnal variation of extraterrestrial (H_o), global (H) and diffuse solar radiation (H_d) at Anantapur during January – December 2013. In the diurnal variation, it shows a steady rise in solar radiation received at the surface after 7:30 LT and attains a maximum solar radiation between 12:00 – 13:00 LT. The amount of solar radiation also varies depending on the time

of day and the season. In general, more solar radiation is present during midday than during either the early morning or late afternoon. At mid-day, the sun is positioned high in the sky and the path of the sun's rays through the earth's atmosphere is shortened. Consequently, less solar radiation is scattered or absorbed, and more solar radiation reaches the earth's surface. [11], [12], [13] observed that the lower values (sunrise and sunset) of solar radiations are due to higher zenith angles, higher atmospheric optics mass and higher distance between the sun to earth, which make the occurrence of greater attenuation of direct radiation by the processes of scattering, absorption, and reflection.

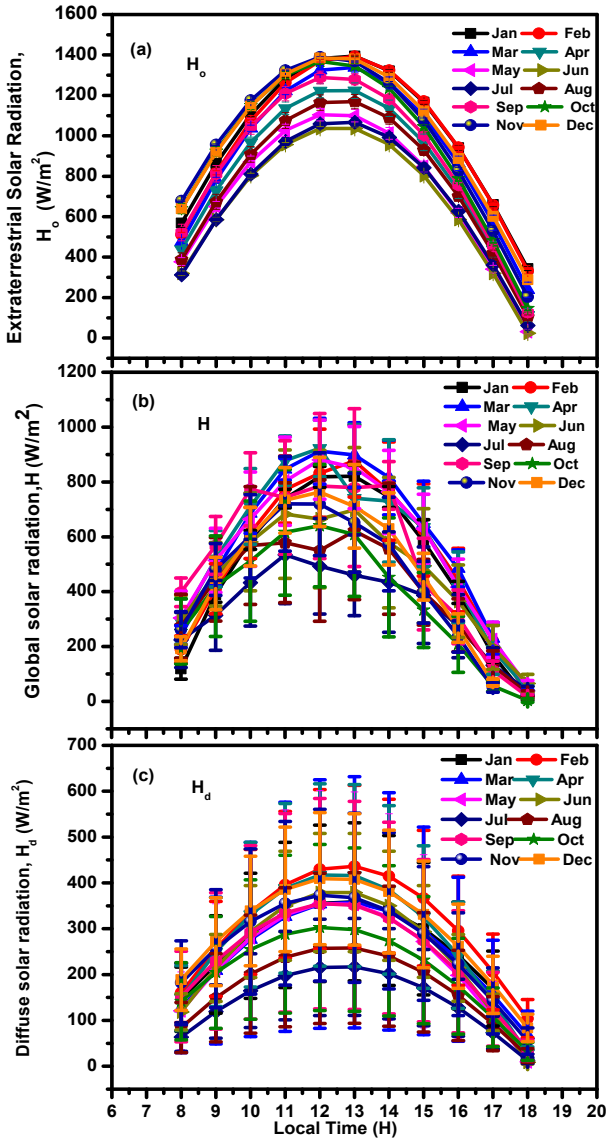

Figure 6: *Diurnal variation of (a) extraterrestrial (b) global and (c) diffuse solar radiation for the entire study period for different months*

In a monthly variation, the solar radiation varies from month to month due to the rotation of the earth as well as local weather conditions. The Figures 7 (a), (b), (c) shows the monthly average of the extraterrestrial solar radiation (H_o), daily global solar radiation (H) and diffuse solar radiation (H_d) on a horizontal surface. The annual mean of daily global, extraterrestrial and diffuse radiation at Anantapur is found to be 202.43 ± 40.45, 408.15 ± 61.63 and 49.33 ± 11.26 W/m^2.

The high global and diffuse solar radiations were observed during March-May (257.67 ± 34.18 W/m^2, 65.07 ± 11.20 W/m^2) whereas low global and diffuse solar radiations are noticed during monsoon

months (137.66 ± 12.41, 33.47 ± 7.44 W/m^2). The high values of global and diffuse solar radiation during summer months are due to clear sky clouds and some aerosol particles that attenuate the incident of solar radiation to the earth's surface. The low values are mainly due to the presence of cloud, rainfall, suspension of water particles that lead to scattering, absorption and reflection of incoming solar radiation to the earth's surface [14]. Extraterrestrial solar radiation was high in the month of December (472.92 ± 0.67 W/m^2) and low in the month of June (312.87 ± 2.58 W/m^2).

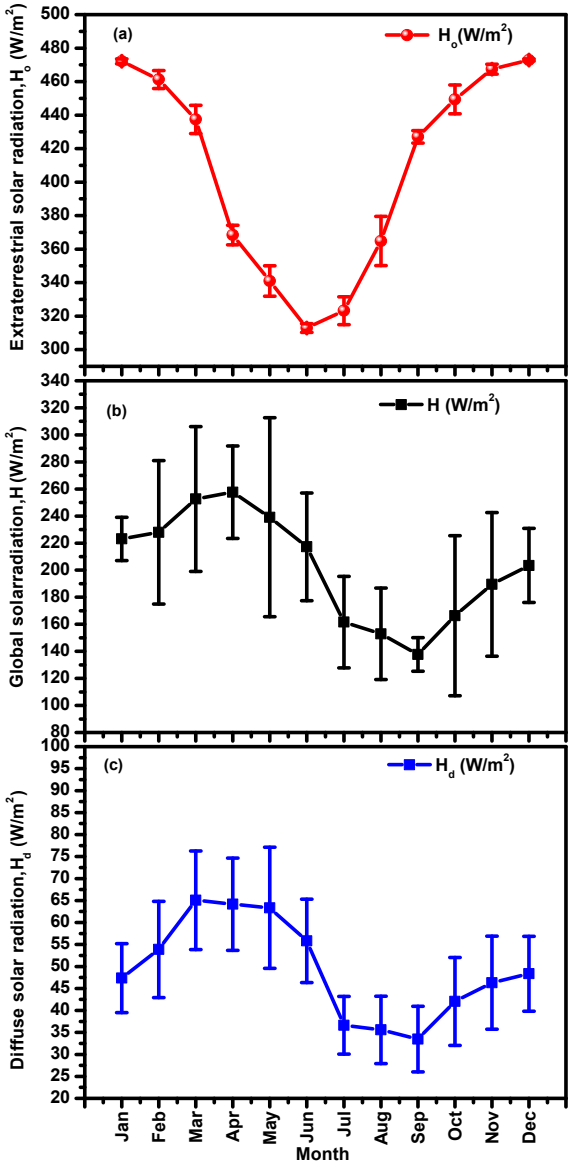

Figure 7: *Monthly variation of (a) extraterrestrial (b) global and (c) diffuse solar radiation*

3.4. Diurnal Variation of Clearness Index (K_t) and Diffuse Index (k_d)

Figures 8 (a), (b) represents the plots of the diurnal variations of monthly mean clearness index (k_t) and diffuse index (k_d) for the period of study. In general clearness index is widely used for the classification of sky conditions. From Figure 8 (a) it is clear that the clearness index was observed low during sunrise and sunset periods and high values at noon. The low values of k_t (0.30 ± 0.14) are mainly due to low global solar radiation and large values of k_t (0.89 ± 0.67) are due to high global solar radiation, which is dominated by the direct component of the radiation. In the case of diffuse

index (k_d), very low values were observed at noon and high values at sunrise and sunset periods. During sunrise and sunset, the solar radiation received at the surface mainly of the diffuse component. This is consistent with the dependence of diffuse solar radiation reaching the surface on solar elevation, atmospheric turbidity, air mass, atmospheric water vapor content and layers and its distribution of cloud cover [15]. During the noon timings, when the sun is over-headed or near over-headed it is noticed that high global radiation may be mainly due to the direct component of radiation.

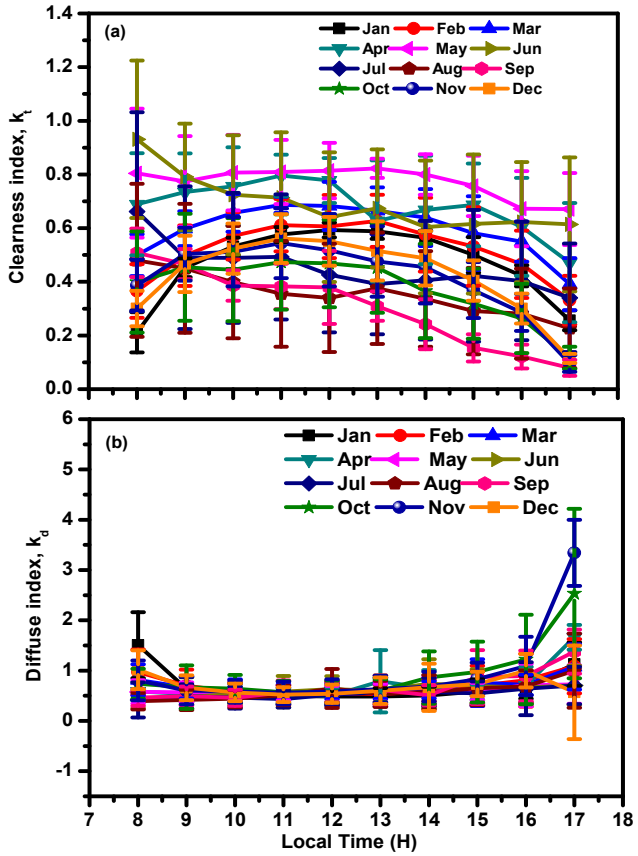

Figure 8: *Diurnal variation of (a) clearness index and (b) diffuse index for different months*

3.5. Monthly Variation of Clearness Index (k_t) and Diffuse Index (k_d)

The monthly variations of the clearness index (k_t) and diffuse index (k_d) for Anantapur throughout the year were shown in Figure 9. The clearness index, k_t is defined as the ratio of the global radiation at ground level on a horizontal surface and the extraterrestrial global solar irradiation [16]. The average values of clearness index and diffuse index were (0.50) and (0.24) respectively for the entire study period. It is observed that the clearness index is during June (0.69) to September (0.32) and then it increases to the maximum in May (0.71). The variation in clearness index is due to the level of humidity and the position of the sun relative to the observation site. The clearness of the sky is generally higher during the summer season. During the northeast monsoon, when both the clearness index and temperatures are low, the global solar radiation is likely to be low, and which is due to the low clearness index and also the solar radiation energy reduces dramatically [17]. The diffuse index maximum and minimum values are observed to be 0.26 (May) and 0.21 (January) respectively [18].

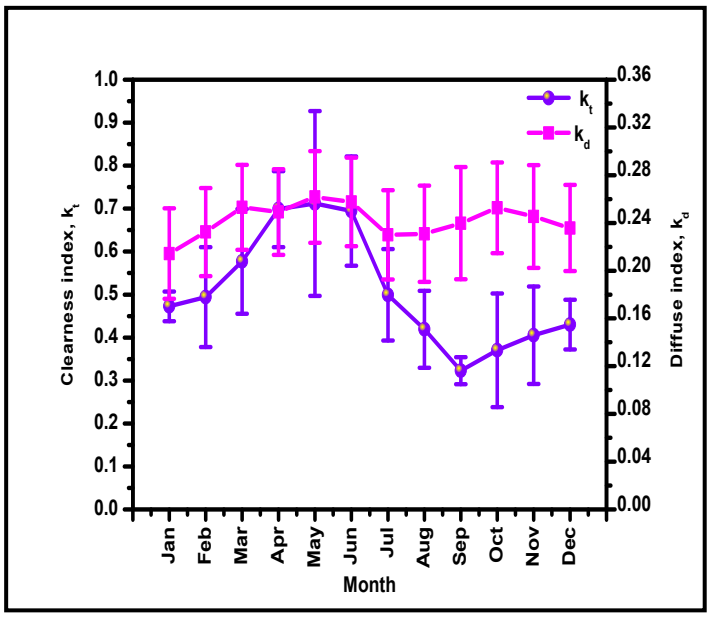

Figure 9: *Monthly variation of clearness index and diffuse index for the entire study period*

3.6. Relationship between Clearness Index (k_t), Diffuse Index (k_d) and Measured Global Solar Radiation (H)

Clearness index (k_t) is a measure of the degree of clearness of the sky and also a measure of solar radiation extinction in the atmosphere, which includes effects due to radiation interaction with other atmospheric constituents [19], [20]. The monthly average values of measured global solar radiation, clearness index and diffuse index are presented in Table 2. Figure 10 (a) shows the positive correlation between global solar radiation (H) and clearness index (k_t). Clearness index is increasing with increasing of global solar radiation and vice versa. It clearly indicates that the maximum values of H and k_t can be harvested in the summer season and minimum values during the monsoon season. In the case of diffuse index, it shows the negative correlation with global solar radiation. Diffuse index found to be low in the month of January (0.21) and high in the month of May (0.26).

Table 2: *The Monthly Average Values of Measured Global Solar Radiation, Clearness Index (K_t) and Diffuse Index (k_d)*

Month	Measured solar radiation (H) (W/m^2)	Extraterrestrial solar radiation (H_o) (W/m^2)	Diffuse solar radiation (H_d) (W/m^2)	Clearness index (k_t) H / H_o	Diffusion index (k_d) H_d / H
Jan	223.084	472.106	47.361	0.472	0.214
Feb	227.966	461.258	53.866	0.494	0.232
Mar	252.628	437.143	65.068	0.577	0.253
Apr	257.669	368.430	64.164	0.698	0.249
May	239.133	340.948	63.347	0.711	0.262
Jun	217.248	312.876	55.829	0.694	0.258
Jul	150.546	323.232	32.569	0.465	0.219
Aug	177.363	364.433	39.863	0.485	0.223
Sep	208.525	422.586	47.686	0.491	0.218
Oct	166.307	449.346	42.046	0.37	0.253
Nov	189.497	467.419	46.303	0.405	0.245
Dec	203.467	472.923	48.340	0.43	0.236

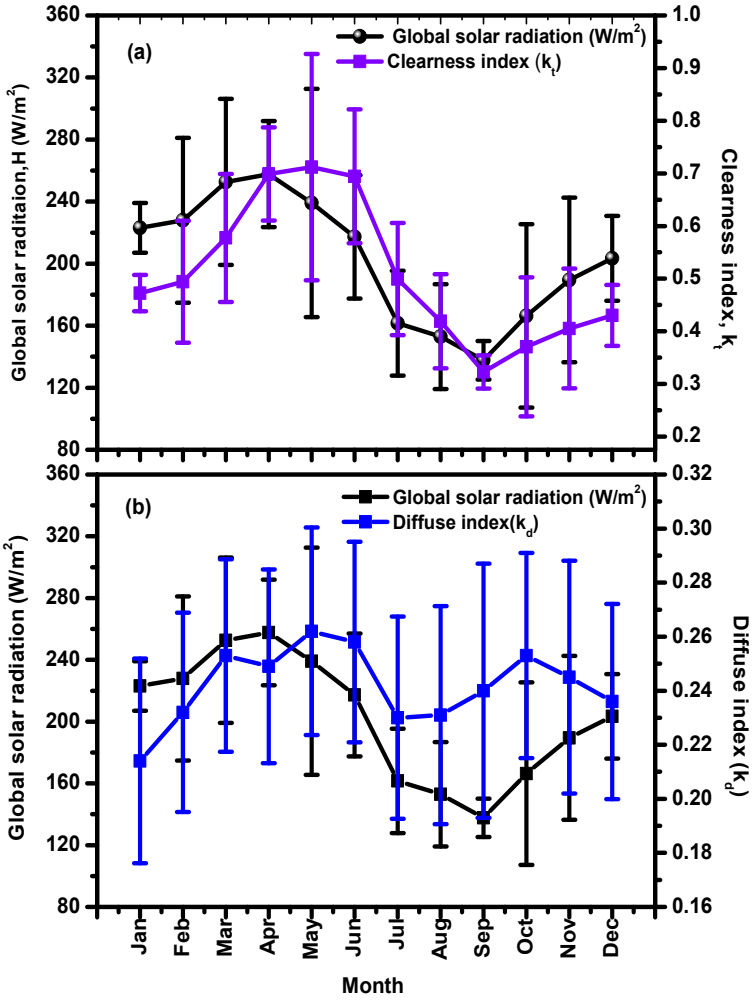

Figure 10: *Relationship between (a) Clearness Index (k_t) and measured global solar radiation (H) and (b) diffuse index (k_d) and measured global solar radiation (H)*

3.7. Variation of Global Solar Radiation with Temperature and Precipitation

The variances of global solar radiation with temperature and precipitation were shown in Figures 11 (a), (b). The maximum temperature was higher in the summer months (April and May) (32.74 ± 3.82 °C and 32.68 ± 3.64 °C) and low in the winter month (25.24 ± 3.43 °C). Higher values of global solar radiation energy recorded in summer months i.e., 386.59 ± 42.56 W/m^2 and lower ones during monsoon months 299.78 ± 53.35 W/m^2 observed in Anantapur. From the Figure 11 (a) it is noticed that in summer, the general trend is that global radiation is high where the temperature is high. In the case of variation of global solar radiation in precipitation, the higher value of precipitation was occurring in the month of September 171.4mm. The distance of the sun rays reached to the earth is smallest during summer, which should result in higher solar radiation. However, the presence of cloud and precipitation reduces the amount of solar radiation received at the ground level [21]. Variations of solar radiation reaching the Earth are thought to influence precipitation, but it is still hard to understand how the periodic variation of solar radiation influences the variation of the precipitation on land, and the extent of this influence on timescales of millennia to decades still remains unclear. It is significant that further investigations and detailed studies of the physical mechanism of solar radiation can probably improve the medium-term and long-term prediction of annual precipitation in the area.

Solar radiation prediction is being paid more attention and the prediction methods are being improved [22].

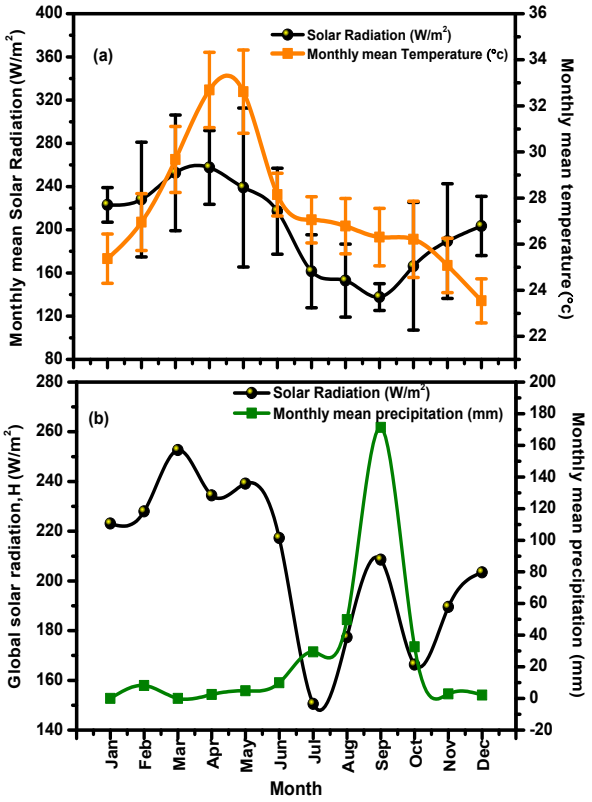

Figure 11: *Variation of global solar radiation with (a) temperature and (b) precipitation*

4. Conclusions

The measurements of meteorological parameters and solar radiation retrieved from MBLM (Mini Boundary Layer Mast) station and Net radiometer sensors during Jan – Dec 2013 was carried out in the present study. These parameters are useful in understanding the energy exchange between land and atmosphere and also helpful to examine the changes in aerosol physical properties and trace gases associated with the changes in prevailing meteorology. The main conclusions drawn from the present study are shown below.

- The minimum temperature of 25.28 ± 3.7 °C was observed during the January 2013 and a maximum of 32.68 ± 3.6 °C during May 2013. The variability in temperature ranges have been found to be 19 - 31, 24 - 38, 23 - 32 and 21 - 30 ^{0}C during winter, summer, monsoon and post monsoon respectively.
- The maximum relative humidity was found to be 76% in the month of September whereas low (36 %) in the month of April.
- The wind speed and directions were measured and the reasons for determining the type of aerosols present over the site and direction from which region they transported are analyzed.
- Diurnal variation of solar radiation shows a steady rise of radiation received at the surface after 7:30 LT and attains a maximum radiation between 12:00 – 13:00 LT.
- The annual means of extraterrestrial, global and diffuse solar radiation was about 408.15 ± 61.63, 202.43 ± 40.45 and 49.33 ± 11.26 W/m^2 respectively.

- The maximum global and diffuse solar radiations were observed during March-May (257.67 ± 34.18 W/m^2, 65.07 ± 11.20 W/m^2) whereas minimum global and diffuse solar radiations are noticed during monsoon months (137.66 ± 12.41, 33.47 ± 7.44 W/m^2).
- The maximum and minimum amount of extraterrestrial solar radiation of 472.92 ± 0.67 W/m^2 and 312.87 ± 2.58 W/m^2 were recorded in December and June respectively.
- The monthly variation of clearness index (k_t) revealed that the month of September has the least value of 0.37 and the month of May has the highest clearness index of 0.71 whereas the diffuse index found to be low in the month of January (0.21) and high in the month of May (0.26).

Acknowledgements

The authors are indebted to Indian Space Research Organization (ISRO), Bangalore for carrying out this work through its Geosphere Biosphere Programme (GBP) under Aerosol Radiative Forcing over India (ARFI) project. We would like to thank NASA's Goddard Earth Sciences Data and Information Services Center.

References

[1] Iziomon, M.G., and Aro, T.O. *The Diffuse Fraction of Global Solar Irradiance at a Tropical Location*. Theoretical and Applied Climatology. 1998. 61; 77-84.

[2] Rao, Kusuma G., Narendra Reddy, N., Ramakrishna, G., Satyanarayana, S., Bhuyan, P.K., Bhuyan, K., Kalita, G., Pathak, B., and Kundu, S.S. 2011: *Field Experiment during the Total Solar Eclipse on 22 July 2009 at Dibrugarh, Monogram.* ISRO Publication, Indian Space Research Organisation, Bangalore, India.

[3] Balakrishnaiah, G., Raghavendra Kumar, K., Suresh Kumar Reddy, B., Swamulu, C., Rama Gopal, K., Reddy, R.R., Reddy, L.S.S., Nazeer Ahammed, Y., Narasimhulu, K., Krishna Moorthy, K., and Suresh Babu, S. *Anthropogenic Impact on the Temporal Variations of Black Carbon and Surface Aerosol Mass Concentrations at a Tropical Semi-Arid Station in Southeastern Region of India*. Journal of Asian Earth Science. 2011. 42; 1297-1308.

[4] Kumar, K.R., Narasimhulu, K., Balakrishnaiah, G., Reddy, B.S.K., Gopal, K.R., Reddy, R.R., Satheesh, S.K., Moorthy, K.K. and Babu, S.S. *Characterization of Aerosol Black Carbon over a Tropical Semi-arid Region of Anantapur, India*. Atmospheric Research. 2011. 100; 12-27.

[5] Ganguly, D., Jayaraman, A., and Gadhavi, H. *Physical and Optical Properties of Aerosols over an Urban Location in Western India: Seasonal Variabilities.* Journal of Geophysical Research. 2006. 111 (D24).

[6] Tessy Chacko, P., and Renuka, G. *Temperature Mapping, Thermal Diffusivity and Subsoil Heat Flux at Kariavattom of Kerala*. Proceedings of the Indian Academy of Sciences – Earth and Planetary Sciences. 2002. 111; 79-85.

[7] Song, Y.M., Guo, W., and Zhang, Y. *Numerical Study of Impacts of Soil Moisture on the Diurnal and Seasonal Cycles of Sensible/Latent Heat Fluxes Over Semi-Arid Region*. Advance in Atmospheric Science. 2009. 26 (2) 319-326.

[8] Rodrıguez-Iturbe, I., Porporato, A., Ridolfi, L., Isham, V., and Cox, D.R. *Probabilistic Modeling of Water Balance at a Point: The Role of Climate, Soil and Vegetation.* Proceedings of the Royal Society of London A. 2000. 455; 3789-3805.

[9] Cheen, S.Q., Lu, S.H., Ao, Y.H., Zhang, Y., Li, S.S., and Shang, L.Y. *Characteristics of Temperature and Moisture of Jinta Oasis in summer under Different Soil Moisture and Weather Conditions*. Journal of Desert Research. 2007. 27 (4) 621-626. (In Chinese)

[10] Guan, X.D., Huang, J.P., Guo, N., Bi, J.R., and Wang, G. *Variability of Soil Moisture and Its Relationship with Surface Albedo and Soil Thermal Parameters over the Loess Plateau.* Advances in Atmospheric Science. 2009. 26 (4) 692-700.

[11] Al-Rawahi, N.Z., Zurigat, Y.H., and Al-Azri, N.A. *Prediction of Hourly Solar Radiation on Horizontal and Inclined Surfaces for Muscat/ Oman*. Journal of Engineering Research. 2011. 8; 19-31.

[12] Teramoto, E.T., and Escobedo, J.F. *Analysis of the Annual Frequency of the Sky Conditions in Botucatu, São Paulo, Brazil.* Revista Brasileira de Engenharia Agrícola e Ambiental. 2012. 16 (9) 985-992.

[13] Souza, A.P., Escobedo, J.F. *Estimates of Hourly Diffuse Radiation on Tilted Surfaces in Southeast of Brazil*. Institute International Journal of Renewable Energy Research. 2013. 3; 1.

[14] Sanusi, Y.K., and Ojo, M.O. *Generation of Clearness Index Maps for Selected Cities in South Western, Nigeria Using Kriging Technique*. International Journal of Humanities, Arts, Medicine and Sciences (IJHAMS). 2015. 3; 1-12.

[15] Okogbue, E.C., Adedokun, J.A., and Holmgren, B. *Hourly and Daily Clearness Index and Diffuse Fraction at a Tropical Station, Ile-Ife, Nigeria*. International Journal of Climatology. 2009. 29; 1035-1047.

[16] Ashok Kumar Rajput, Rajesh Kumar Tewari, and Atul Sharma. *Utility Base Estimated Solar Radiation at Destination Pune, Maharashtra, India*. International Journal of Pure and Applied Sciences and Technology. 2012. 13 (1) 19-26.

[17] Abdul Majeed Muzathik, Wan Mohd Norsani Bin Wan Nik, Khalid Bin Samo, and Mohd Zamri Ibrahim. *Reference Solar Radiation Year and Some Climatology Aspects of East Coast of West Malaysian* American Journal of Engineering and Applied Sciences. 2010. 3 (2) 293-299.

[18] Hassan A.N. Hejase, and Ali H. Assi, 2014: *Estimation of Global and Diffuse Horizontal Irradiance in Abu Dhabi, United Arab Emirates*. 13th World Renewable Energy Congress (WREC XIII), London, UK.

[19] Falayi, E.O., Rabiu, A.B., and Teliat, R.O. *Correlations to Estimate Monthly Mean of Daily Diffuse Solar Radiation in Some Selected Cities in Nigeria*. Advances in Applied Science Research. 2011. 2 (4) 480-490.

[20] Ndilemeni, C.C., Momoh, M., and Akande, J.O. *Evaluation of Clearness Index of Sokoto Using Estimated Global Solar Radiation.* IOSR Journal of Environmental Science, Toxicology and Food Technology (IOSR-JESTFT). 2013. 5; 51-54.

[21] Poudyal, K.N., Bhattarai, B.K., Sapkota, B.K., Berit Kjeldstad, and Karki, N.R. *Estimation of Global Solar Radiation using Pyranometer and NILU-UV Irradiance Meter at Pokhara Valley in Nepal*. Journal of the Institute of Engineering. 2014. 9; 69-78.

[22] Wang, B., and Ho, L. *Rainy Season of the Asian-Pacific Summer Monsoon*. Journal of Climatology. 2002. 15; 386-398.